Few-Body Syst (2011) 49: 121–128
DOI 10.1007/s00601-010-0111-y

S. G. Bondarenko · V. V. Burov · E. P. Rogochaya

Covariant Relativistic Separable Kernel Approach for Electrodisintegration of the Deuteron at High Momentum Transfer

Relativistic Description of Two- and Three-Body Systems in Nuclear Physics, ECT*, October 13–19 2009

Received: 31 July 2010 / Accepted: 14 October 2010 / Published online: 29 October 2010

Abstract The paper considers the electrodisintegration of the deuteron for kinematic conditions of the JLab experiment E-94-019. The calculations have been performed within the covariant Bethe–Salpeter approach with a separable kernel of nucleon–nucleon interactions. The results have been obtained using the relativistic plane wave impulse approximation and compared with experimental data and other models. The influence of nucleon electromagnetic form factors has been investigated.

1 Introduction

New experimental data for exclusive electrodisintegration of the deuteron at high momentum transfer [1] can be a good instrument for testing proposed relativistic models of nucleon–nucleon (NN) interactions. The specific arrangement of the experiment when the final state interaction (FSI) effects are minimized allows one to compare results of the calculations performed within the plane wave impulse approximation (PWIA). Therefore, there is a chance to investigate the influence of nucleon momentum distributions produced by various models describing observables.

During last 15 years several relativistic models of NN interactions have been elaborated [2–6]. Generally, they are based on fully relativistic expressions for matrix elements depending on four-momenta of the nucleons under consideration. However, in most cases there are difficulties caused by the necessity to perform calculations with the zeroth component of nucleon relative momentum p_0. They are solved by using some constraints on p_0 obtained from physical assumptions that limits the applicability of these models to low-energy calculations. In practice, they are based on using nonrelativistic nuclear interaction models (realistic [7,8] or separable potentials [9,10]). The attempt to apply the covariant separable kernel [11,12] fails because of nonintegrable singularities which appear when calculations in the high energy region are performed. This problem was solved in [13–15] where the fully relativistic covariant model was elaborated. Now it is interesting to investigate how this model describes the electrodisintegration of the deuteron at high momentum transfer where relativistic effects are assumed to play an important role.

Another interesting problem is the influence of the used proton and neutron electromagnetic form factors. The widely used model is the dipole fit [16]. However, it is well known and intensively discussed that the

S. G. Bondarenko · V. V. Burov · E. P. Rogochaya (✉)
Bogoliubov Laboratory of Theoretical Physics, Joint Institute for Nuclear Research,
Dubna, Russia
E-mail: rogoch@theor.jinr.ru; rogoch@yandex.ru

S. G. Bondarenko
E-mail: bondarenko@jinr.ru

V. V. Burov
E-mail: burov@theor.jinr.ru

relation of proton charge form factor G_{Ep} to the proton magnetic form factor G_{Mp} obtained by the Rosenbluth separation technique, differs from the one obtained by the recoil polarization method [17,18]. To describe the results of the latter method, it is necessary to use parametrization [17] for G_{Ep}. It should be noted that in this case the Galster parametrization for the neutron electric form factor G_{En} [19] is applied [2]. In this paper we compare the calculations with the original dipole fit for the proton and neutron form factors with those where the modified G_{Ep} and G_{En} are used.

The paper is organized as follows. The formalism to describe NN interactions within the Bethe–Salpeter approach with a separable interaction kernel is presented in Sect. 2. Section 3 considers the calculated cross section. The obtained results are discussed in Sect. 4.

2 Formalism

In the paper the deuteron electrodisintegraton is considered within the Bethe–Salpeter (BS) approach [20] with a separable kernel of NN interactions. It is based on the solution of the BS equation:

$$\Phi^{JM}(k;\,K) = \frac{i}{(2\pi)^4} S_2(k;\,K) \int d^4p V(k,\,p;\,K)\Phi^{JM}(p;\,K) \tag{1}$$

for the bound state of the neutron–proton (np) system with the total angular momentum J and its projection M described by the BS amplitude Φ^{JM}. Here the total $K = k_p + k_n$ and the relative $k = (k_p - k_n)/2$ momenta are used instead of the proton k_p and neutron k_n momenta. In general, the BS amplitude can be decomposed by the partial-wave states through the generalized spherical harmonic $\mathcal{Y}$ and the radial part ϕ [12] as:

$$\Phi^{JM}_{\alpha\beta}\left(k;\,K_{(0)}\right) = \sum_a \left(\mathcal{Y}_{aM}(\mathbf{k})U_C\right)_{\alpha\beta}\ \phi_a\left(k_0,\,|\mathbf{k}|\right), \tag{2}$$

where $K_{(0)} = (M_d, \mathbf{0})$ is the total momentum of the NN system in its rest frame (here it is the deuteron rest frame called the laboratory system, LS); M_d is the mass of the deuteron; U_C is the charge conjugation matrix; α, β denote matrix indices; a is a short notation of the partial-wave state $^{2S+1}L^{\rho}_{J}$ with spin S, orbital L and total J angular momenta, ρ means positive- or negative-energy partial-wave state. $S_2(k;\,K)$ is the free two-particle Green function:

$$S_2^{-1}(k;\,K) = \left(\tfrac{1}{2}\,K\cdot\gamma + k\cdot\gamma - m\right)^{(1)}\left(\tfrac{1}{2}\,K\cdot\gamma - k\cdot\gamma - m\right)^{(2)}.$$

In these calculations it is more convenient to use the BS vertex function Γ^{JM} which is connected with the BS amplitude by the following relation:

$$\Phi^{JM}(k;\,K) = S_2(k;\,K)\Gamma^{JM}(k;\,K). \tag{3}$$

After using the decomposition of type (2) for the vertex function the relation between the Φ^{JM} and Γ^{JM} radial parts can be deduced:

$$\phi_a(k_0,\,|\mathbf{k}|) = \sum_b S_{ab}(k_0,\,|\mathbf{k}|;\,s)g_b(k_0,\,|\mathbf{k}|), \tag{4}$$

where S_{ab} is the one-nucleon propagator [12]. To solve the BS equation (1), we have used the separable ansatz for the interaction kernel

$$V_{ab}(p_0,\,|\mathbf{p}|;\,k_0,\,|\mathbf{k}|;\,s) = \sum_{i,j=1}^{N} \lambda_{ij}(s)g_i^{[a]}(p_0,\,|\mathbf{p}|)g_j^{[b]}(k_0,\,|\mathbf{k}|), \tag{5}$$

where N is a rank of the kernel, g_i are model functions; λ is a parameter matrix satisfying the symmetry property $\lambda_{ij}(s) = \lambda_{ji}(s)$; $k[p]$ is the relative momentum of the initial [final] nucleons; $s = (p_p + p_n)^2$ where p_p is the outgoing proton and p_n is the neutron momentum, respectively. If the radial part of the vertex function Γ^{JM} is written in the following form:

$$g_a(p_0,\,|\mathbf{p}|) = \sum_{i,j=1}^{N} \lambda_{ij}(s)g_i^{[a]}(p_0,\,|\mathbf{p}|)c_j(s), \tag{6}$$

the initial integral BS equation (1) is transformed into a system of linear homogeneous equations for the coefficients $c_i(s)$:

$$c_i(s) - \sum_{k,j=1}^{N} h_{ik}(s)\lambda_{kj}(s)c_j(s) = 0, \tag{7}$$

where

$$h_{ij}(s) = -\frac{i}{4\pi^3}\sum_a \int dk_0 \int \mathbf{k}^2 d|\mathbf{k}| \frac{g_i^{[a]}(k_0,|\mathbf{k}|)g_j^{[a]}(k_0,|\mathbf{k}|)}{(\sqrt{s}/2 - E_{\mathbf{k}} + i\epsilon)^2 - k_0^2} \tag{8}$$

and $E_{\mathbf{k}} = \sqrt{\mathbf{k}^2 + m^2}$. Using (4) and taking into account only positive-energy partial-wave states for the deuteron ${}^3S_1^+, {}^3D_1^+$, the radial part of the BS amplitude can be written as follows:

$$\phi_a(k_0,|\mathbf{k}|) = \frac{g_a(k_0,|\mathbf{k}|)}{(M_d/2 - E_{\mathbf{k}} + i\epsilon)^2 - k_0^2}. \tag{9}$$

Thus, using separable g functions we can calculate observables describing the np system.

3 Cross Section

When all particles are unpolarized the exclusive $d(e,e'n)p$ process can be described by the cross section in LS:

$$\begin{aligned}\frac{d^3\sigma}{dQ^2 d|\mathbf{p}_n| d\Omega_n} = \frac{\sigma_{\text{Mott}}\pi \mathbf{p}_n^2}{2(2\pi)^3 M_d E_e E'_e}\big[&l_{00}^0 W_{00} + l_{++}^0(W_{++} + W_{--}) + l_{+-}^0 \cos 2\phi\ 2\text{Re}W_{+-} \\ &- l_{+-}^0 \sin 2\phi\ 2\text{Im}W_{+-} - l_{0+}^0 \cos\phi\ 2\text{Re}(W_{0+} - W_{0-}) \\ &- l_{0+}^0 \sin\phi\ 2\text{Im}(W_{0+} + W_{0-})\big],\end{aligned} \tag{10}$$

where $\sigma_{\text{Mott}} = (\alpha \cos\frac{\theta}{2}/2E_e \sin^2\frac{\theta}{2})^2$ is the Mott cross section, $\alpha = e^2/4\pi$ is the fine structure constant; E_e $[E'_e]$ is the energy of the initial [final] electron; Ω'_e is the outgoing electron solid angle; θ is the electron scattering angle; $Q^2 = -q^2 = -\omega^2 + \mathbf{q}^2$, where $q = (\omega, \mathbf{q})$ is the momentum transfer. The outgoing neutron is described by momentum $\mathbf{p}_n$ and solid angle $\Omega_n = (\theta_n, \phi)$ with zenithal angle θ_n between $\mathbf{q}$ and $\mathbf{p}_n$ momenta and azimuthal angle ϕ between the $(\mathbf{ee}')$ and $(\mathbf{qp}_n)$ planes. The photon density matrix elements have the following form:

$$\begin{aligned} l_{00}^0 &= \frac{Q^2}{\mathbf{q}^2}, \quad l_{0+}^0 = \frac{Q}{|\mathbf{q}|\sqrt{2}}\sqrt{\frac{Q^2}{\mathbf{q}^2} + \tan^2\frac{\theta}{2}}, \\ l_{++}^0 &= \tan^2\frac{\theta}{2} + \frac{Q^2}{2\mathbf{q}^2}, \quad l_{+-}^0 = -\frac{Q^2}{2\mathbf{q}^2}. \end{aligned} \tag{11}$$

The hadron density matrix elements

$$W_{\lambda\lambda'} = W_{\mu\nu}\varepsilon_\lambda^\mu \varepsilon_{\lambda'}{}^\nu, \tag{12}$$

where λ, λ' are photon helicity components [21], can be calculated using the photon polarization vectors ε and Cartesian components of hadron tensor

$$W_{\mu\nu} = \frac{1}{3}\sum_{s_d s_n s_p} \left| < np : SM_S | j_\mu | d : 1M > \right|^2, \tag{13}$$

where S is the spin of the np pair and M_S is its projection. The hadron current j_μ in (13) can be written according to the Mandelstam technique [22] and has the following form:

$$\langle np : SM_S|j_\mu|d : 1M\rangle = i\sum_{r=1,2}\int\frac{d^4p}{(2\pi)^4}\mathrm{Sp}\left\{\Lambda(\mathcal{L}^{-1})\bar{\psi}_{SM_S}(p^{\mathrm{CM}};P^{\mathrm{CM}})\Lambda(\mathcal{L})\right.$$
$$\left.\times\Gamma_\mu^{(r)}(q)S^{(r)}\left(\frac{K_{(0)}}{2}-(-1)^r p-\frac{q}{2}\right)\Gamma^M\left(p+(-1)^r\frac{q}{2};K_{(0)}\right)\right\} \quad (14)$$

within the relativistic impulse approximation. The sum over $r = 1, 2$ corresponds to the interaction of the virtual photon with the proton and with the neutron in the deuteron, respectively. Total P^{CM} and relative p^{CM} momenta of the outgoing nucleons are considered in the final np pair rest frame (center-of-mass system, CM) and can be written in LS using the Lorenz-boost transformation along the $\mathbf{q}$ direction. The Lorenz transformation of np pair wave function ψ_{SM_S} from CM to LS is:

$$\Lambda(\mathcal{L}) = \left(\frac{1+\sqrt{1+\eta}}{2}\right)^{\frac{1}{2}}\left(1+\frac{\sqrt{\eta}\gamma_0\gamma_3}{1+\sqrt{1+\eta}}\right), \quad (15)$$

where $\eta = \mathbf{q}^2/s$. The interaction vertex is chosen in the on-mass-shell form:

$$\Gamma_\mu(q) = \gamma_\mu F_1(q^2) - \frac{1}{4m}\left(\gamma_\mu\hat{q}-\hat{q}\gamma_\mu\right)F_2(q^2), \quad (16)$$

here $F_1(q^2)$ is the Dirac form factor, $F_2(q^2)$—Pauli form factor. The form factors are described by the dipole fit model [16] or modified dipole fit [17,19]. If the outgoing nucleons are supposed to be non-interacting then this is the so-called plane-wave approximation. In this case the np pair wave function can be written in the following form:

$$\bar{\psi}_{SM_S}(p;P) \to \bar{\psi}^{(0)}_{SM_S}(p,p^*;P) = (2\pi)^4\bar{\chi}_{SM_S}(p;P)\delta(p-p^*), \quad (17)$$

where $p^* = (0, \mathbf{p}^*)$ is the relative momentum of on-mass-shell nucleons, χ_{SM_S} describes spinor states of the pair. Taking into account representation (17), the hadron current (14) can be transformed into a sum:

$$\langle np : SM_S|j_\mu|d : 1M\rangle = i\sum_{r=1,2}\left\{\Lambda(\mathcal{L}^{-1})\bar{\chi}_{SM_S}\left(p^{*\mathrm{CM}};P^{\mathrm{CM}}\right)\Lambda(\mathcal{L})\Gamma_\mu^{(r)}(q)\right.$$
$$\left.\times S^{(r)}\left(\frac{K_{(0)}}{2}-(-1)^r p^*-\frac{q}{2}\right)\Gamma^M\left(p^*+(-1)^r\frac{q}{2};K_{(0)}\right)\right\}. \quad (18)$$

In this paper the cross section of the exclusive electrodisintegration of the deuteron $d^2\sigma/dQ^2d|\mathbf{p}_n|$ [1] is calculated. It can be obtained from (10) after integration over the neutron solid angle:

$$\frac{d^2\sigma}{dQ^2d|\mathbf{p}_n|} = \int\limits_{\Omega_n}\frac{d^3\sigma}{dQ^2d|\mathbf{p}_n|d\Omega_n}d\Omega_n. \quad (19)$$

According to [1] the integration is performed over $\Omega_n : 20^\circ \leqslant \theta_n \leqslant 160^\circ, 0^\circ \leqslant \phi \leqslant 360^\circ$. Four different Q^2 are considered. The obtained results are discussed in the next section.

4 Results and Discussion

In this paper the exclusive cross section of electrodisintegration (19) for kinematic conditions of the JLab experiment [1] has been calculated within the Bethe–Salpeter approach with the rank-six separable kernel MY6 [15]. The calculations have been performed within the relativistic PWIA. The obtained results have been compared with experimental data and two theoretical models, the nonrelativistic Graz II (NR) [23] and relativistic Graz II [11] separable interaction kernels.

Figures 1, 2, 3, 4 illustrate the cross section depending on outgoing neutron momentum $\mathbf{p}_n$ for $Q^2 = 2, 3, 4, 5\,\mathrm{GeV}^2$, respectively. The dipole fit model [16] for the nucleon electromagnetic form factors has been

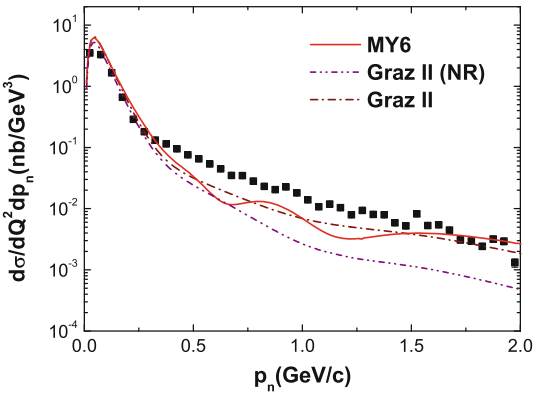

Fig. 1 The cross section (19) depending on neutron momentum $\mathbf{p}_n$ is considered for $Q^2 = 2 \pm 0.25\,\mathrm{GeV}^2$. Calculations with the Graz II (NR) [23] (*dash-dot-dotted line*), Graz II [11] (*dash-dotted line*) and MY6 [15] (*solid line*) models are present. The dipole fit model [16] for nucleon form factors is used

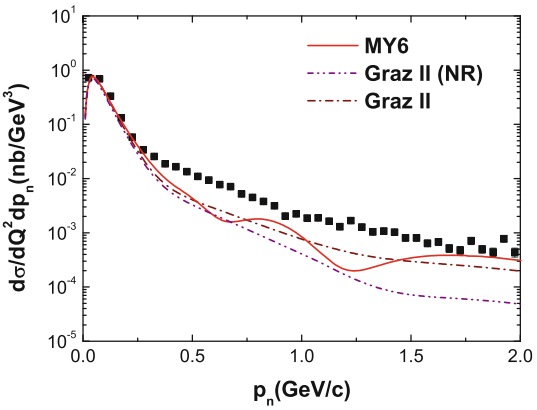

Fig. 2 As in Fig.1, but for $Q^2 = 3 \pm 0.5\,\mathrm{GeV}^2$

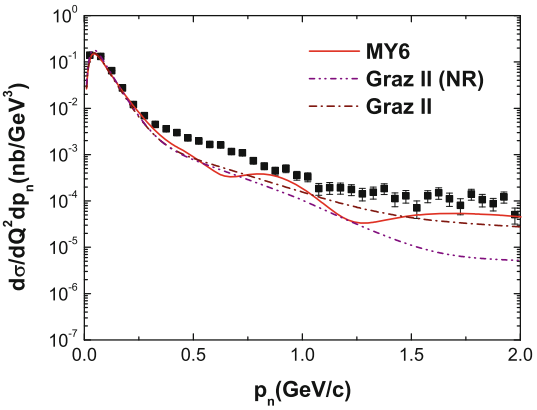

Fig. 3 As in Fig.1, but for $Q^2 = 4 \pm 0.5\,\mathrm{GeV}^2$

used. One nonrelativistic Graz II (NR) and two relativistic MY6, Graz II separable kernels of NN interactions have been investigated. A good agreement with the experimental data can be seen at low neutron momenta $|\mathbf{p}_n| < 0.25\,\mathrm{GeV/c}$ on the figures. The discrepancy between the theoretical models and the experimental data increases with $|\mathbf{p}_n| > 0.25\,\mathrm{GeV/c}$ for all the considered models. However, we see the agreement of the relativistic models (MY6, Graz II) with the experimental data at high neutron momenta. Moreover, the relativistic description becomes better with Q^2 increasing and theoretical curves go practically along experimental points

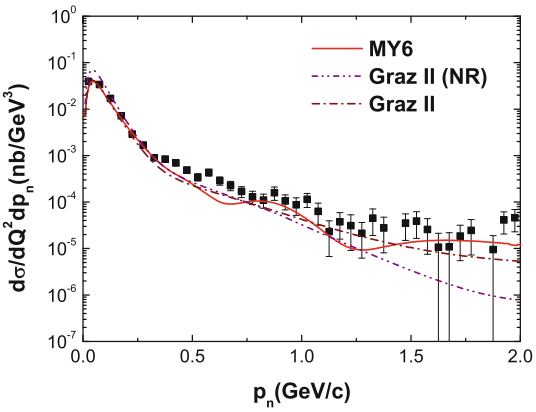

Fig. 4 As in Fig.1, but for $Q^2 = 5 \pm 0.5\,\mathrm{GeV}^2$

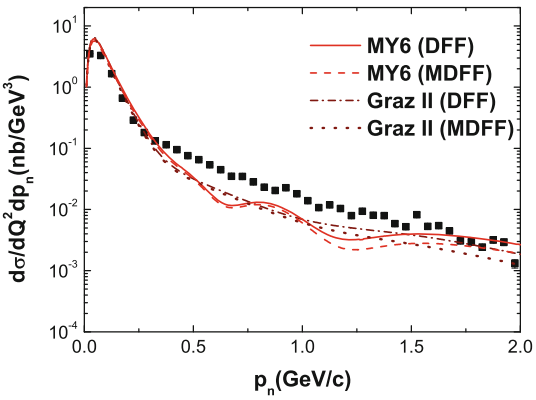

Fig. 5 The calculated cross sections (19) by using the dipole fit model for nucleon electromagnetic form factors [16] [MY6 (DFF)—*solid line*, Graz II (DFF)—*dash-dotted line*] are compared to those obtained with modified G_{Ep} [17] and G_{En} [19] [MY6 (MDFF)—*dashed line*, Graz II (MDFF)—*dotted line*]. $Q^2 = 2 \pm 0.5\,\mathrm{GeV}^2$

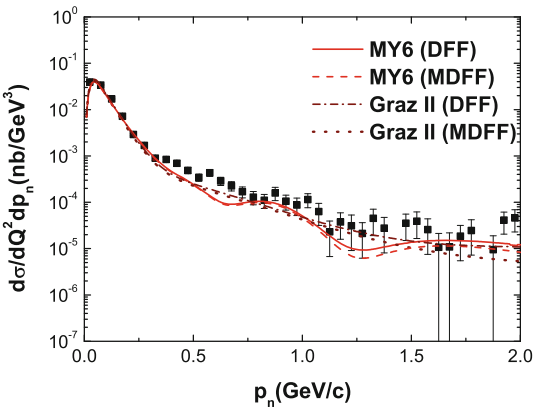

Fig. 6 As in Fig.5, but for $Q^2 = 5 \pm 0.5\,\mathrm{GeV}^2$

at $Q^2 = 5\,\mathrm{GeV}^2$. Therefore, relativistic effects play an important role in description of the deuteron electrodisintegration at high momentum transfer and high neutron momenta.

The calculations with the modified proton G_{Ep} [17] and neutron G_{En} [19] form factors at $Q^2 = 2\,\mathrm{GeV}^2$ (Fig. 5) and $Q^2 = 5\,\mathrm{GeV}^2$ (Fig. 6) are compared to those obtained using the dipole fit model for nucleon form factors. Two relativistic models of NN interactions MY6 and Graz II have been considered. All the theoretical calculations agree with the experiment at $|\mathbf{p}_n| < 0.25\,\mathrm{GeV/c}$ and begin to deviate from it with $\mathbf{p}_n$ increasing. We can also see slight difference between the cross sections obtained using the dipole fit and modified dipole

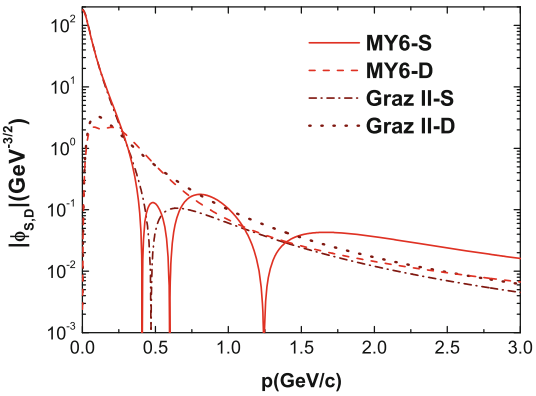

Fig. 7 The radial parts of the amplitude (9) for the ${}^3S_1^+$ and ${}^3D_1^+$ partial-wave states at $k_0 = M_d/2 - E_{\mathbf{k}}$ are presented. They are written in the deuteron rest frame. The MY6 model [15] (MY6-S *solid line* corresponds to ${}^3S_1^+$ partial-wave state, MY6-D *dashed line*—to ${}^3D_1^+$) is compared with Graz II [11] (Graz II-S *dash-dotted line*—${}^3S_1^+$ wave function, Graz II-D *dotted line*—${}^3D_1^+$ wave function)

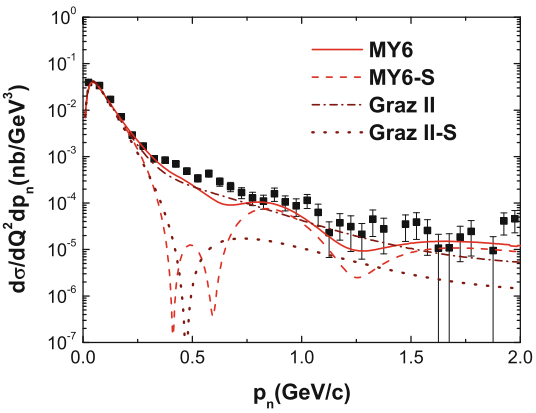

Fig. 8 The contribution of the ${}^3S_1^+$ partial-wave state to the cross section (19) is shown. Calculations with (MY6 *solid* and Graz II *dash-dotted lines*) and without the ${}^3D_1^+$ state (MY6-S *dashed* and Graz II-S *dotted lines*) in the deuteron are compared at $Q^2 = 5 \pm 0.5\,\mathrm{GeV}^2$

fit models for the nucleon electromagnetic form factors. It is interesting that the results calculated within the dipole fit model, which does not describe the behavior of the electric form factor of the proton at high Q^2, are virtually undistinguishable from those obtained with the modified G_{Ep} [17]. However, the final conclusion which model is better can be made only when the final state interactions, negative-energy partial-wave states (P waves) and two-body currents (TBC) are taken into account.

It should be noted that the behavior of the calculated cross section is similar to the behavior of the corresponding wave function for the deuteron ${}^3S_1^+$ partial-wave state which is shown in Fig. 7. It is seen from the comparison of the cross sections calculated with (MY6, Graz II) and without ${}^3D_1^+$ partial-wave state (MY6-S, Graz II-S) in the deuteron (Fig. 8) that the influence of the ${}^3S_1^+$ state is maximum at low and medium neutron momenta. The minima of the ${}^3S_1^+$ wave functions are noticeable in the cross section. They are smoothed by the ${}^3D_1^+$ state when the both partial-wave states are taken into account. The role of the ${}^3D_1^+$ state increases at high $\mathbf{p}_n$.

It is seen from Figs. 1, 2, 3, 4, 5, 6 that the Graz II and MY6 models give qualitatively the similar description of the experimental data within the used approximation. The difference between the model calculations and the experimental data can be probably eliminated when FSI, P waves and TBC are taken into account. It should be emphasized that there is no possibility to improve a theoretical description using the Graz II model. As it was mentioned above, FSI is impossible to calculate with the Graz II kernel for high-energy particles unless the p_0 component is constrained by some assumption like, for instance, in quasipotential approaches. On the contrary, it is possible to take FSI into account using the MY6 kernel without constraining p_0.

We should also comment the results obtained using the Paris potential model [8] in [1]. A good agreement with the experimental data was achieved when the FSI and meson-exchange current effects were taken into account. However, it seems questionable to use the nonrelativistic potential elaborated to describe the np elastic scattering data for laboratory energies of the colliding particles less than 350 MeV when the cross section at high Q^2 and $|\mathbf{p}_n|$ is calculated. The MY6 model has two important advantages. Firstly, it is fitted to describe all available elastic np scattering data [15]. Secondly, it allows one to perform calculations without any necessity to constrain p_0 [13–15].

In this paper the comparison of three different models of NN interactions has demonstrated that relativistic effects play an important role in the description of the deuteron electrodisintegration at high momentum transfer. The result is slightly dependent of the model used for the proton and neutron electromagnetic form factors. Further investigation is required to conclude which models of NN interactions and nucleon electromagnetic form factors are reasonable. In particular, it is necessary to calculate FSI, P waves and so on.

Acknowledgments Authors would like to thank the organizers of "Relativistic Description of Two- and Three-Body Systems in Nuclear Physics" Workshop for an opportunity to present and discuss this work. Speaker R.E.P. is grateful to them for their warm hospitality.

References

1. Egiyan, K.S. et al.: the CLAS: Experimental study of exclusive ^{2}H(e,e′p)n reaction mechanisms at high Q^2. Phys. Rev. Lett. **98**, 262502 (2007) [nucl-ex/0701013]
2. Laget, J.M.: The electro-disintegration of few body systems revisited. Phys. Lett. **B609**, 49–56 (2005) [nucl-th/0407072]
3. Frankfurt, L.L., Sargsian, M.M., Strikman, M.I.: Feynman graphs and generalized eikonal approach to high energy knock-out processes. Phys. Rev. **C56**, 1124–1137 (1997) [nucl-th/9603018]
4. Karmanov, V.A., Carbonell, J.: Solving Bethe–Salpeter equation in Minkowski space. Eur. Phys. J. A **27**, 1 (2006) [hep-th/0505261]; Eur. Phys. J. A **27**, 11 (2006) [hep-th/0505262]
5. Jeschonnek, S., Van Orden, J.W.: Origin of relativistic effects in the reaction D(e,e′p)n at GeV energies. nucl-th/9911063 (1999)
6. Arriaga, A., Schiavilla, R.: A relativistic calculation of the deuteron threshold electrodisintegration at backward angles. Phys. Rev. **C76** 014007 (2007) [0704.2514 [nucl-th]]
7. Machleidt, R.: The high-precision, charge-dependent Bonn nucleon–nucleon potential (CD-Bonn). Phys. Rev. C **63**, 024001 (2001)
8. Lacombe, M. et al.: Parametrization of the Paris N-N Potential. Phys. Rev. C **21**, 861 (1980)
9. Plessas, W.: On-shell and Off-shell Behavior of Separable Nucleon Nucleon Potentials. Acta Phys. Austriaca **54**, 305 (1982)
10. Kwong, N.H., Kohler, H.S.: Separable NN potentials from inverse scattering for nuclear matter studies. Phys. Rev. C **55**, 1650 (1997)
11. Rupp, G., Tjon, J.A.: Relativistic contributions to the deuteron electromagnetic form factors. Phys. Rev. C **41**, 472 (1990)
12. Bondarenko, S.G., Burov, V.V., Molochkov, A.V., Smirnov, G.I., Toki, H.: Bethe–Salpeter approach with the separable interaction for the deuteron. Prog. Part. Nucl. Phys. **48**, 449–535 (2002) [nucl-th/0203069]
13. Bondarenko, S.G., Burov, V.V., Rogochaya, E.P., Yanev, Y.: (2008) 0806.4866 [nucl-th]
14. Bondarenko, S.G., Burov, V.V., Pauchy Hwang, W.-Y., Rogochaya, E.P.: Relativistic multirank interaction kernels of the neutron–proton system. Nucl. Phys. A **832**, 233 (2010) [nucl-th/0612071]
15. Bondarenko, S.G., Burov, V.V., Pauchy Hwang, W.-Y., Rogochaya, E.P.: Covariant separable interaction for the neutron–proton system in $^3S_1 - ^3D_1$ partial-wave state. 1002.0487 [nucl-th]
16. Pietschmann, H., Stremnitzer, H.: Nucleon form factors and asymptotic symmetries. Lett. Nuovo Cim. **2**, 841 (1969)
17. Gayou, O. et al.: Jefferson Lab Hall A: Measurement of G_{Ep}/G_{Mp} in $\overrightarrow{e}\,\mathrm{p} \to \mathrm{e}\,\overrightarrow{\mathrm{p}}$ to $Q^2 = 5.6\,\mathrm{GeV}^2$. Phys. Rev. Lett. **88**, 092301 (2002) [nucl-ex/0111010]
18. Jones, M.K. et al. (Jefferson Lab Hall A): G_{Ep}/G_{Mp} ratio by polarization transfer in $\overrightarrow{e}\,\mathrm{p} \to \mathrm{e}\,\overrightarrow{\mathrm{p}}$. Phys. Rev. Lett. **84**, 1398 (2000) [nucl-ex/9910005]
19. Galster, S. et al.: Elastic electron–deuteron scattering and the electric neutron form-factor at four momentum transfers $5\,\mathrm{fm}^{-2} < q^2 < 14\,\mathrm{fm}^{-2}$. Nucl. Phys. B **32**, 221–237 (1971)
20. Salpeter, E.E., Bethe, H.A.: A Relativistic equation for bound state problems. Phys. Rev. **84**, 1232 (1951)
21. Dmitrasinovic, V., Gross, F.: Polarization observables in deuteron photodisintegration and electrodisintegration. Phys. Rev. C **40**, 2479 (1989)
22. Mandelstam, S.: Dynamical variables in the Bethe–Salpeter formalism. Proc. Roy. Soc. Lond. A **233**, 248 (1955)
23. Mathelitsch, L., Plessas, W., Schweiger, W.: Separable potential for the neutron–proton system. Phys. Rev. C **26**, 65 (1982)